S1-NMR. Protonation sequence of L12-L15 ligands **25 July 2017**

^{1}H-NMR measurements were carried out in order to support the deprotonation sequence[1] identified for all the ligands by potentiometric titration and UV-Vis measurements, to better define the deprotonation steps and to give evidence of some related structural rearrangements. ^{1}H-NMR spectra were collected for all the ligands in the pH range 1.4-13 (Figures 1-NMR, 5-NMR, 9-NMR and 13-NMR, upper parts).

For L12 ligand, the intrinsic chemical shifts[2] for all the protons and their variations related to each deprotonation step are collected in Table 1. The trends of chemical shifts *vs* pH of all the protons are shown in Figure 1-NMR.

The first deprotonation step $LH_3 \rightarrow LH_2^-$ mainly affects P and M aromatic protons and in a smaller amount N and E protons, supporting that the first deprotonation process involves the carboxylic group of the molecule.

Table 1-NMR. Intrinsic chemical shifts (calculated by HypNMR) of the protons of L12 ligand in the different protonated species and variations of the intrinsic chemical shifts related to each deprotonation step.

Species	**E**	**F**	**G**	**L**	**M**	**N**	**P**
$\mathbf{L^{3-}}$	6,50	6,33	4,20	6,94	7,24	7,23	7,28
$\mathbf{LH^{2-}}$	6,27	6,42	4,38	7,27	7,29	7,29	7,35
$\mathbf{LH_2^-}$	6,66	6,48	4,32	7,25	7,32	7,34	7,45
$\mathbf{LH_3}$	6,76	6,49	4,29	7,29	7,52	7,45	7,88
Δδ	**E**	**F**	**G**	**L**	**M**	**N**	**P**
$\mathbf{LH^{2-} \rightarrow L^{3-}}$	-0,23	0,10	0,17	0,33	0,04	0,06	0,07
$\mathbf{LH_2^- \rightarrow LH^{2-}}$	0,39	0,05	-0,05	-0,02	0,04	0,05	0,11
$\mathbf{LH_3 \rightarrow LH_2^-}$	0,10	0,01	-0,03	0,04	0,20	0,11	0,42

[1] We prefer to describe the deprotonation sequence in order to follow the trend of chemical shifts *vs* increasing pH.
[2] The intrinsic chemical shift is the chemical shift of each differently protonated species present in the system, calculated by HypNMR program.

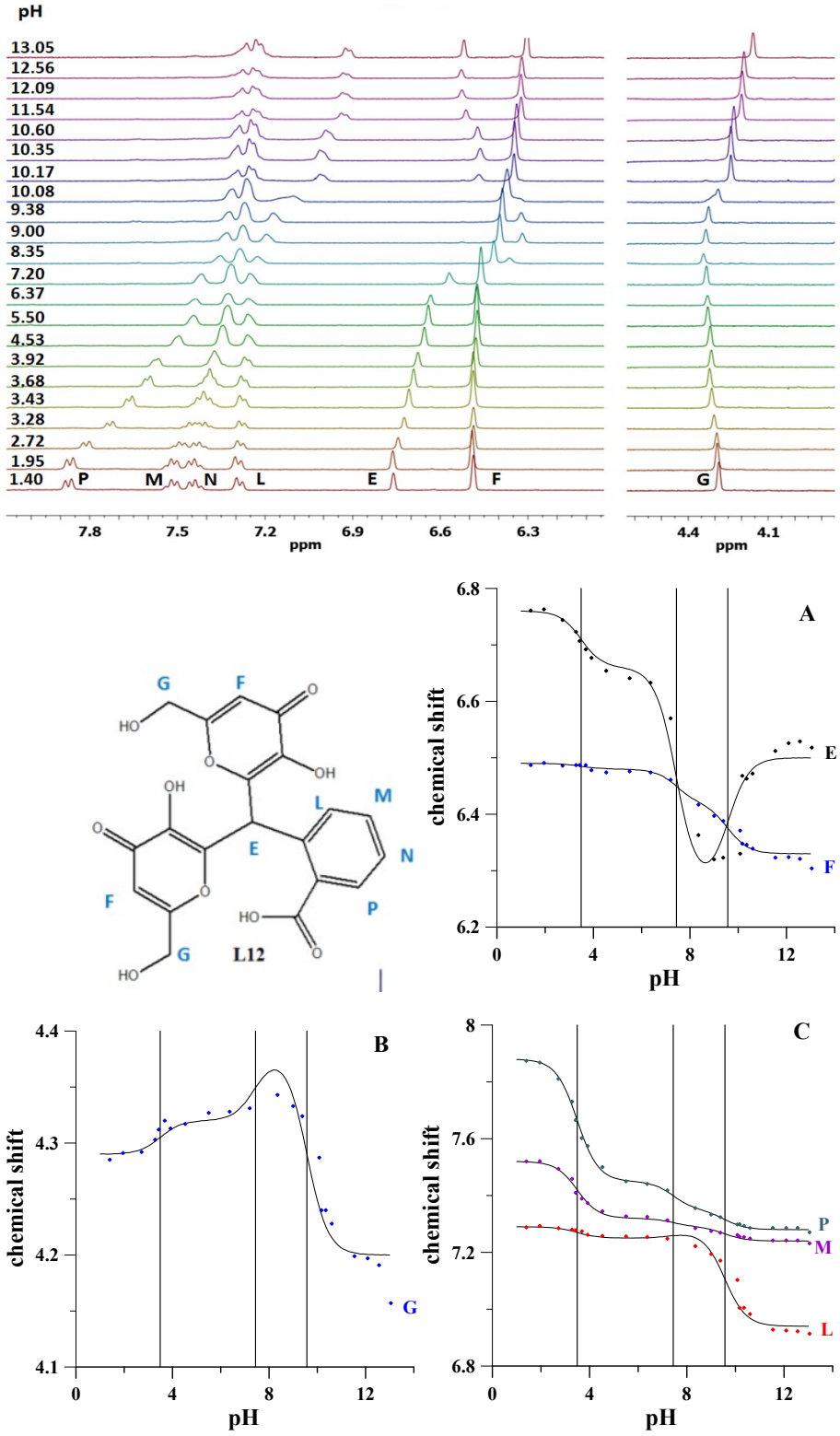

Figure 1-NMR. (Upper Figure) ^{1}H NMR spectra of L12 at increasing pH (1.95-13.05). (Lower Figure) Chemical shifts variation for the protons E, F, G, P, M and L of L12 ligand *vs.* pH. Three continuous grid lines are reported in correspondence of the three pK values.

The protons in ortho and para position to COOH group are those mainly affected, as shown in Figure 1. The formation of a hydrogen bond, which involves the oxygen from the deprotonated carboxylic group COO^- and the OH group in the KA ring, implies a conformational change that affects the E proton on the linker (Figure 1 A, B, C and Figure 2).

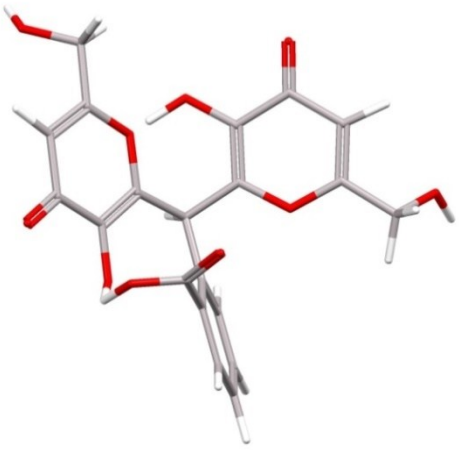

Figure 2-NMR. Hydrogen bond formation $COO^{-}\cdots HO$, after the deprotonation of the carboxylic group in the first step.

The deprotonation of OH group of one KA moiety in the second step $LH_2^- \rightarrow LH^{2-}$, strongly affects the chemical shift of the signal of the proton E on the linker. The proton F in meta to the OH group, is only slightly affected by the deprotonation. The large change in the intrinsic chemical shift of E proton could originate from the breaking of $COO^{-}\cdots HO$ hydrogen bond, and the formation of a new hydrogen bond $O^-\ldots HO$ between the two KA units. The breaking of the previous $COO^{-}\cdots HO$ hydrogen bond also affects the resonance of P, no more involved in a hydrogen bond (Figure 1C).

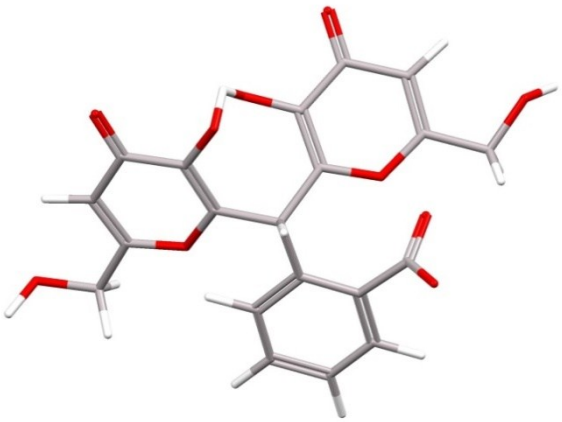

Figure 3-NMR. Hydrogen bond formation $O^{-}HO$ between the two KA units.

The third step $LH^{2-} \rightarrow L^{3-}$ involves the deprotonation of the OH group on the second KA unit. The $O^{-}\cdots HO$ hydrogen bond is no more possible, and the molecule rearranges to form new hydrogen

bonds involving the hydroxymethyl groups, one with the carboxylic group and the second with the OH of the KA moiety (Figure 4). This fact reverses the direction of the chemical shift of E proton towards lower field, and affects the resonance of G protons and that of the aromatic L proton (Figure 1C).

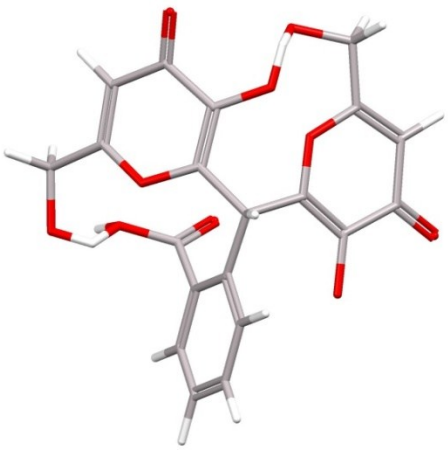

Figure 4-NMR. Hydrogen bond formation after the third deprotonation step of L12 ligand.

The intrinsic chemical shifts of L13 protons and the variations of the intrinsic chemical shifts connected to each deprotonation step are reported in Table 2-NMR. Also L13 ligand undergoes the loss of the proton from carboxylic group in the first deprotonation. The first step strongly affects signals of I and, in a smaller amount, of L aromatic proton, and no indication of a hydrogen bond $COO^{-}\cdots HO$- formation is observed (Figure 5-NMR A, B, C, and Figure 6).

Table 2-NMR. Intrinsic chemical shifts (calculated by HypNMR) of the protons of L13 ligand in the different protonated species and variations of the intrinsic chemical shifts related to each deprotonation step.

Species	**E**	**F**	**G**	**I**	**L**
$\mathbf{L^{3-}}$	6,43	6,34	4,28	7,72	7,21
$\mathbf{LH^{2-}}$	6,07	6,42	4,36	7,75	7,31
$\mathbf{LH_2^{-}}$	6,20	6,49	4,35	7,76	7,36
$\mathbf{LH_3}$	6,22	6,49	4,34	7,93	7,43
Δδ	**E**	**F**	**G**	**I**	**L**
$\mathbf{LH^{2-}\rightarrow L^{3-}}$	-0,36	0,08	0,07	0,03	0,10
$\mathbf{LH_2^{-}\rightarrow LH^{2-}}$	0,13	0,07	-0,01	0,02	0,05
$\mathbf{LH_3\rightarrow LH_2^{-}}$	0,02	0,00	-0,01	0,17	0,07

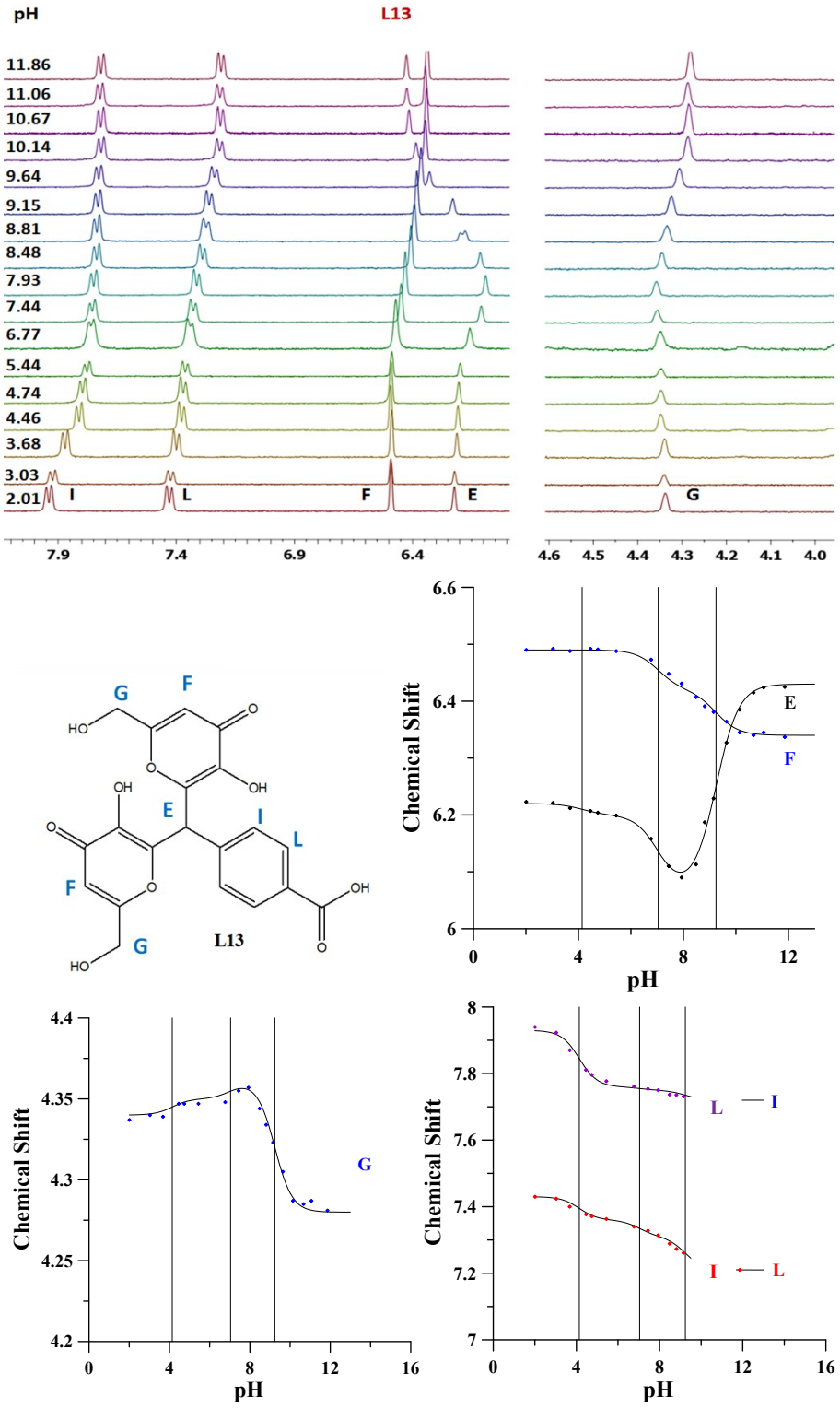

Figure 5-NMR. (Upper Figure) ^{1}H NMR spectra of L13 at increasing pH (2.01-11.86). (Lower Figure) Chemical shifts of F, E, G, L and I protons of L13 ligand *vs.* pH. Three continuous grid lines are reported in correspondence of the three pK values.

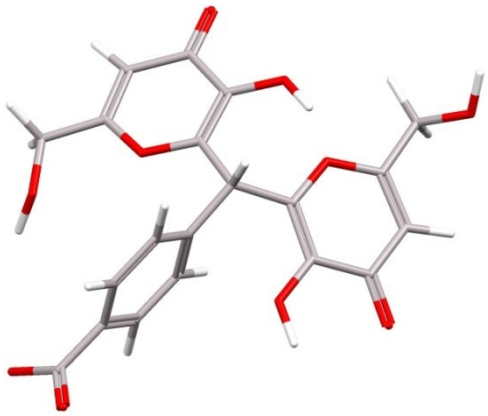

Figure 6-NMR. L13 ligand after the loss of the H on the carboxylic group.

In the second deprotonation step the signal of proton E on the linker is the most affected, suggesting that the deprotonation of one –OH group leads to a hydrogen bond OH---$^{-}$O between the two units of KA. Figure 7-NMR shows a model of the molecule after the formation of the hydrogen bond OH---$^{-}$O between the two units of KA.

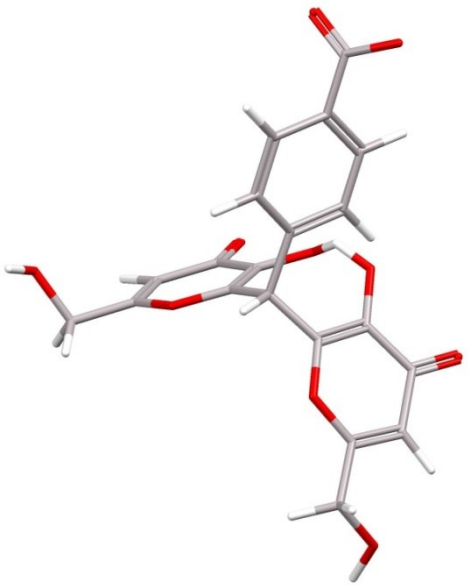

Figure 7-NMR. Hydrogen bond OH---$^{-}$O between the two units of KA after the second deprotonation of L13 ligand.

The hydrogen bond between the two KA moities breaks when the third deprotonation occurs. This last step involves the deprotonation of the second OH group. In this condition a hydrogen bond ispossible, between O^{-} in one KA unit with CH_2OH in the second (Figure 8-NMR). This implies

imply a large torsion of the E proton on the linker, and consequently large chemical shift variations for F, G and L signals have been determined (Figure 5-NMR).

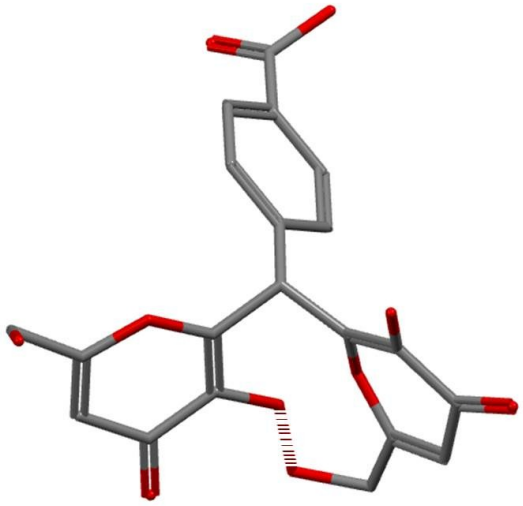

Figure 8-NMR. Hydrogen bond formation after the third deprotonation of L13 ligand.

The intrinsic chemical shifts for the L14 protons and the variations of the intrinsic chemical shifts related to each deprotonation step are reported in Table 3-NMR. Figure 9-NMR shows the variations of chemical shifts of L14 protons as a function of pH.

Table 3-NMR. Intrinsic chemical shifts (calculated by HypNMR) of the protons of L14 ligand in the different protonated species and variations of the intrinsic chemical shifts related to each deprotonation step.

Species	**E**	**F**	**G**	**I**	**L**	**M**	**N**
L^{3-}	6,32	6,34	4,29	6,99	6,53	7,05	6,64
LH^{2-}	6,20	6,37	4,38	7,32	6,88	7,17	6,87
LH_2^-	6,09	6,45	4,35	7,15	6,86	7,20	6,85
LH_3	6,30	6,50	4,33	7,12	6,89	7,23	6,91
Δδ	**E**	**F**	**G**	**I**	**L**	**M**	**N**
$LH^{2-} \rightarrow L^{3-}$	-0,11	0,03	0,09	0,34	0,34	0,12	0,23
$LH_2^- \rightarrow LH^{2-}$	-0,11	0,07	-0,04	-0,17	-0,02	0,02	-0,02
$LH_3 \rightarrow LH_2^-$	0,21	0,05	-0,02	-0,04	0,04	0,03	0,06

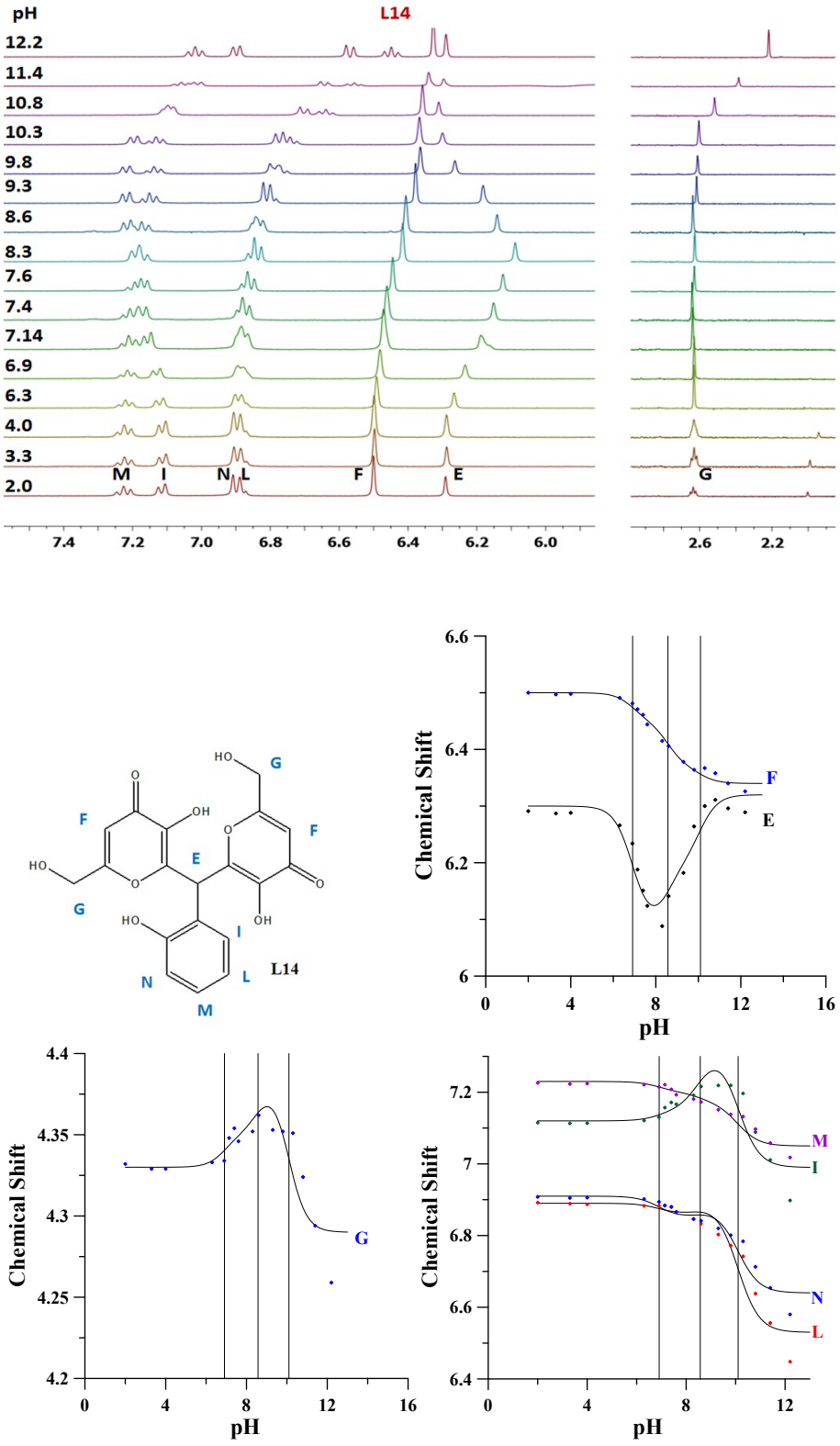

Figure 9-NMR. (Upper Figure) ^{1}H NMR spectra of L14 at increasing pH (2.0-12.2). (Lower Figure) Chemical shift variations of F, E, G, M, I, N and L protons of L14 ligand *vs.* pH. Three continuous grid lines are reported in correspondence of the three pK values.

The first and the second deprotonation, as observed from the UV spectra collected during L14 titration, involve the OH groups on the KA units. The first deprotonated oxygen atom can form hydrogen bonds either with the OH group of the phenol moiety in the linker (Figure 10-NMR A), or with the OH group in the second KA unit (Figure 10-NMR B). The chemical shifts related to the signal attributed to N proton supports the first hypothesis, confirmed by the relevant chemical shifts related to E signal on the linker, which in this case undergoes a strong rotation around the bond.

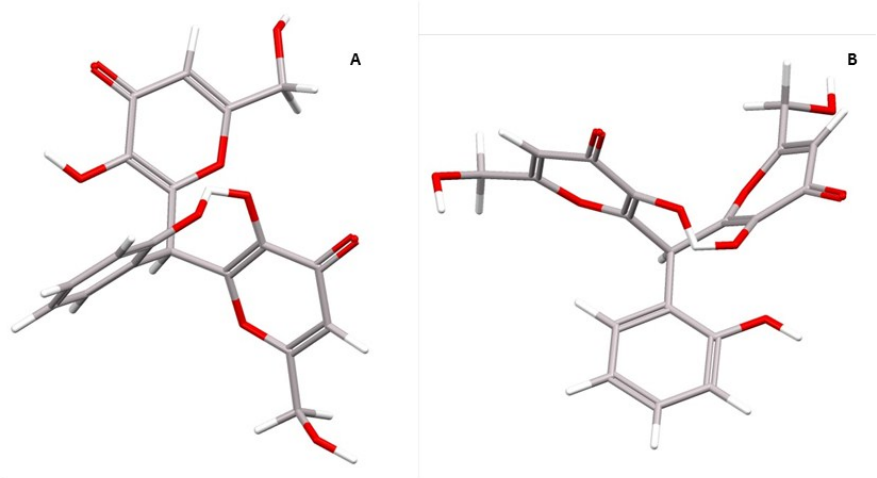

Figure 10-NMR. The two hypothesis of hydrogen bond formation after the first deprotonation involving L14 ligand.

After the second deprotonation an opposite chemical shift towards lower field takes place on the signal of E proton; this fact is probably due to the formation of a hydrogen bond OH---$^{-}$O with the CH_2OH group on the second KA unit. (Figure 11-NMR).

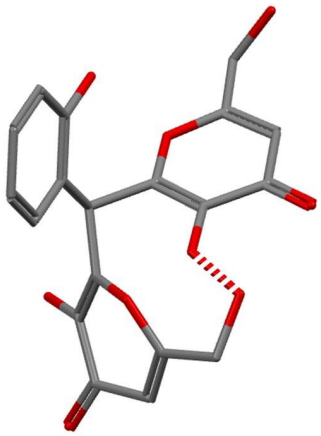

Figure 11-NMR. Hydrogen bond formation after the second deprotonation step of L14 ligand.

The third deprotonation affects the intrinsic chemical shifts of all the signals attributed to the protons of the phenolic moiety, and of the E proton on the linker as shown in Figure 9-NMR. The

formation of a hydrogen bond is possible between the phenate group and one CH_2OH group of the KA moiety (Figure 12-NMR).

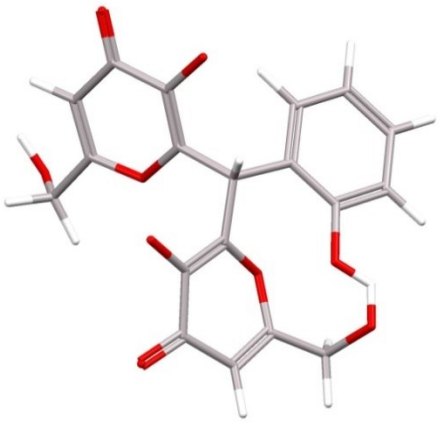

Figure 12-NMR. Hydrogen bond between $-O^-$ from the phenolic group and CH_2OH on one of the KA units after the third deprotonation step of L14 ligand.

The intrinsic chemical shifts of L15 protons and the variations of the intrinsic chemical shifts related to each deprotonation step, are reported in Table 4-NMR. Figure 13-NMR shows the chemical shifts of L15 protons as a function of pH.

Table 4-NMR. Intrinsic chemical shifts (calculated by using HypNMR) of the different protons in L15 ligand in the different protonated species, and variations of the intrinsic chemical shifts related to each deprotonation step.

Species	**E**	**F**	**G**	**I**	**L**
$\mathbf{L^{3-}}$	6,26	6,32	4,31	6,91	6,50
$\mathbf{LH^{2-}}$	6,17	6,37	4,33	7,11	6,78
$\mathbf{LH_2^-}$	5,94	6,44	4,37	7,19	6,80
$\mathbf{LH_3}$	6,07	6,48	4,35	7,21	6,82
Δδ	**E**	**F**	**G**	**I**	**L**
$\mathbf{LH^{2-} \rightarrow L^{3-}}$	-0,09	0,04	0,03	0,20	0,28
$\mathbf{LH_2^- \rightarrow LH^{2-}}$	-0,23	0,07	0,03	0,08	0,01
$\mathbf{LH_3 \rightarrow LH_2^-}$	0,12	0,04	-0,01	0,03	0,02

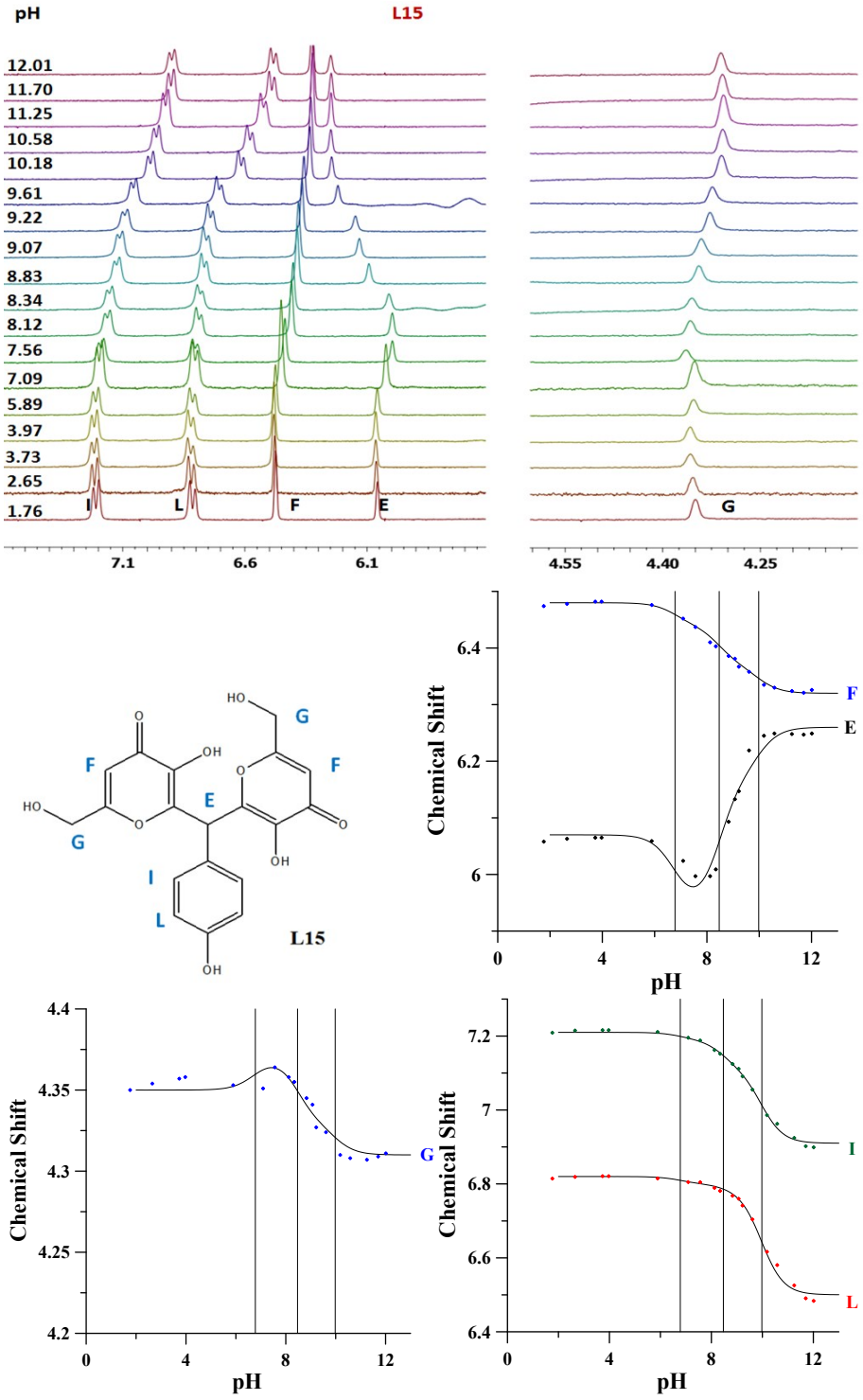

Figure 13-MR. (Upper Figure) ^{1}H NMR spectra of L15 at increasing pH (1.73-12.01).
(Lower Figure) Chemical shifts variations for F, E, G, I and L protons of L15 ligand *vs*. pH. Three continuous grid lines are reported in correspondence of the three pK values.

The first and the second deprotonation involve the OH groups of the KA units. The first deprotonated hydroxyl group can form a hydrogen bond only with the OH group located in the second KA unit (Figure 14-NMR).

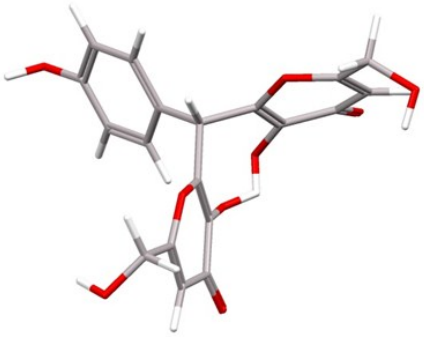

Figure 14-NMR. Hydrogen bond -OH---$^{-}$O between the two KA units of L15 ligand.

After the second deprotonation, an opposite chemical shift towards lower field involves the signal attributed to the E proton on the linker. This behavior is related to the formation of a hydrogen bond with the CH_2OH group on the second KA unit (Figures 15-NMR).

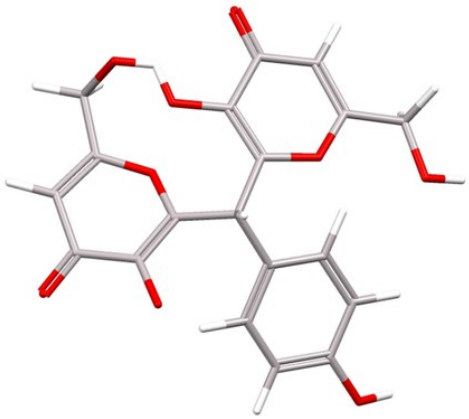

Figure 15-NMR. Hydrogen bond OH---$^{-}$O with the CH_2OH on the second KA unit after the second deprotonation of L15 ligand.

The third deprotonation affects the intrinsic chemical shifts of all the protons of the phenolic unit, together with the E proton. The only possible hydrogen bond involves the deprotonated hydroxyl group in the KA unit and one of the CH_2OH group (Figures 16-NMR).

Figure 16-NMR. Hydrogen bond OH---O with the CH_2OH on the second KA unit after the third deprotonation step of L15 ligand.